# Prediction of Activation Energies for Aromatic Oxidation by Cytochrome P450†

**Patrik Rydberg,‡ Ulf Ryde,§ and Lars Olsen*,‡**

*Department of Medicinal Chemistry, Copenhagen University, Universitetsparken 2, DK-2100 Copenhagen, Denmark, and the Department of Theoretical Chemistry, Lund University, P.O. Box 124, SE-22100 Lund, Sweden*

*Received: May 1, 2008; Revised Manuscript Received: September 12, 2008*

We have estimated the activation energy for aromatic oxidation by compound I in cytochrome P450 for a diverse set of 17 substrates using state-of-the-art density functional theory (B3LYP) with large basis sets. The activation energies vary from 60 to 87 kJ/mol. We then test if these results can be reproduced by computationally less demanding methods. The best methods (a B3LYP calculation of the activation energy of a methoxy-radical model or a partial least-squares model of the semiempirical AM1 bond dissociation energies and spin densities of the tetrahedral intermediate for both a hydroxyl-cation and a hydroxyl-radical model) give correlations with $r^2$ of 0.8 and mean absolute deviations of 3 kJ/mol. Finally, we apply these simpler methods on several sets of reactions for which experimental data are available and show that we can predict the reactive sites by combining calculations of the activation energies with the solvent-accessible surface area of each site.

## Introduction

The cytochromes P450 (CYPs) form a ubiquitous protein family with functions including synthesis and degradation of many physiologically important compounds, as well as degradation of xenobiotic compounds, for example, drugs.[1] Much effort has been put into the study of these enzymes, because they influence the transformation of prodrugs into their active form, as well as the bioavailability and degradation of many drugs.

The CYP enzymes catalyze several different types of reactions, of which the oxidation of aromatic and alkene $sp^2$-hybridized carbon atoms are two of the most important. The mechanisms of these reactions have been studied both experimentally[2−4] and theoretically,[5−9] showing that the first step involves the formation of a tetrahedral intermediate, in which the oxygen of the reactive heme $Fe^{V}$═O species (formally), called compound I, is bound to the carbon atom of the substrate.[2] The formation of this intermediate has been predicted to be the rate-limiting step.[10] From this intermediate, there are two possible reaction paths (Scheme 1). Either an epoxide is formed through a simple ring closure, in which the oxygen atom binds to a neighboring carbon atom, or a short-lived intermediate is formed, in which a hydrogen atom is transferred to a nitrogen atom on the porphyrin ring[7] (a so-called NIH shift[11,12]). The NIH-shift intermediate can then rearrange into several different products (alcohol, ketone, or aldehyde). After the tetrahedral intermediate is formed, a third possibility exists if the substrate is an alkene, namely that a carbon atom in the substrate binds to a pyrrole nitrogen atom, forming a suicide complex.

Considering the importance of the CYPs in the metabolism of drugs, it would be highly desirable to have a method that could predict if and in what way a drug candidate will be metabolized by these enzymes. Most previous studies have been focused on how a compound is metabolized, based on quantum chemical studies on isolated substrates, pharmacophore models, docking, molecular dynamics simulations, chemical rules, statistical algorithms, or quantitative structure−activity relationships (QSAR) from physicochemical, topological, or 3D structures.[13−18] The consensus is that no single computational approach can reliably predict metabolism by the CYPs. Instead, a combination of both the intrinsic reactivity of various parts of the substrate (electronic factors) and the accessibility of the groups to the reactive $Fe^{V}$═O group in the enzyme (steric effects) need to be taken into account.[13,19]

The intrinsic reactivity of the various groups has normally been estimated by quantum mechanical (QM) methods at the Hartree−Fock, semiempirical, or DFT levels. For oxidation of aromatic carbon atoms, the intrinsic reactivity has been estimated

**SCHEME 1: Possible Reaction Paths in Oxidation of Benzene by the CYPs**

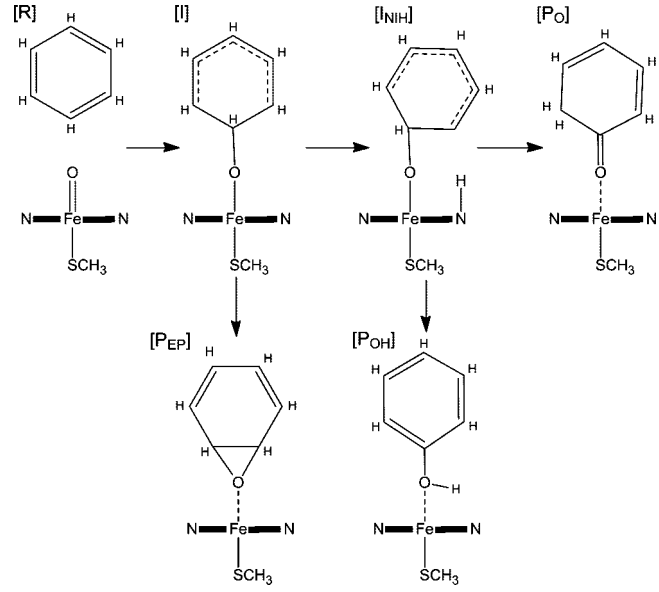


† Part of the "Sason S. Shaik Festschrift".

* To whom correspondence should be addressed. Phone: (+45) 35 30 63 05, Fax: (+45) 35 30 60 40, E-mail: lo@farma.ku.dk.
‡ Copenhagen University.
§ Lund University.

10.1021/jp803854v CCC: $40.75 
Published on Web 11/06/2008

from the stability of the tetrahedral intermediate[15,20,21] or from statistical data.[20] It has also been estimated from the hydrogen-abstraction energy, alone[22] or combined with the solvent-accessible surface area,[17,18,23] which is somewhat surprising, because there is no hydrogen abstraction in the reaction mechanism of aromatic oxidation. More sophisticated methods involve the direct estimation of the activation energy of the reactions by use of a simplified models of the $Fe^{V}$═O state of CYP, for example a methoxy radical.[15] Recently, it has even become possible to calculate activation energies with DFT and full models of the active porphyrin species, giving nearly quantitative results.[6−8,10,24−27] However, such calculations are quite time consuming, especially for molecules of the size of a typical drug (weeks of CPU time). On the other hand, they can be used to develop and calibrate more approximate methods. Two such attempts have been published[10,24] but they used only substituted benzenes as substrates and tested relatively few methods.

In this article, we extend this work and show that previous semiempirical models have serious deficiencies. We find that energies calculated with a methoxy radical at the DFT level as well as bond dissociation energies calculated using the semiempirical AM1 method with hydroxyl−radical and hydroxyl−cation models can be used to predict state-of-the-art DFT energies as well as experimental data. The methods work equally well for both aromatic and alkene $sp^2$-hybridized carbon atoms.

## Computational Methodology

We have modeled compound I of the CYPs as iron (formally $Fe^{V}$) porphine (i.e., a porphyrin without side chains) with $CH_3S^-$ and $O^{2-}$ (formally) as axial ligands. Two states along the reaction path were studied (Scheme 1), namely the isolated compound I and substrate, and the transition state for the oxidation. Reported activation energies are the energy difference of these two states, if not otherwise stated. We also tested to model compound I by a methoxy radical, as has been done before.[15,28,29] In that case, we studied also the reactant complex, that is, the complex of the substrate and the methoxy radical, and the intermediate after the oxidation, in which the oxygen atom of the product is still weakly bound to the iron atom. Finally, we also studied the tetrahedral intermediate using both a hydroxyl-radical or a hydroxyl-cation model of compound I, as has been previously suggested.[24]

The quantum chemical calculations were performed with the density functional method B3LYP[30−32] (unrestricted formalism for open-shell systems) or with the semiempirical AM1 method.[33] In the B3LYP calculations, we have used for iron the double-ζ basis set of Schäfer et al.,[34] enhanced with a p function with the exponent 0.134915. For the other atoms, the 6−31G(d) basis set[35−37] was used. The final energies were determined with B3LYP using the 6−311++G(2d,2p) basis set[38] for all atoms, except iron, for which we used the double-ζ basis set of Schäfer et al.,[34] enhanced with s, p, d, and *f* functions (exponents of 0.01377232, 0.041843, 0.1244, 2.5, and 0.8; two *f* functions).[39] This basis set combination is denoted BSII below. These energies also include the zero-point vibrational energy, calculated at the B3LYP/6−31G(d) level. The frequency calculations also verified that the structures were true minima or transition states. Solvent effects where not considered because Bathelt et al. have shown that this does not affect the relative activation energies for reactions of the type studied in this article.[24]

The aim of this article is to see if various cheaper theoretical methods can reproduce the final DFT activation energies. This is done by determining the coefficient of determination ($r^2$) and the mean absolute deviations (MAD) between the results of the various methods and the DFT energies. The MAD was calculated after a linear-regression analysis.

The B3LYP calculations with the compound I model were performed with the *Turbomole 5.9* software,[40,41] whereas all other calculations were performed with the *Gaussian 03* software.[42] Multivariate analysis was performed using the *SIMCA-P* software, version 11.0 (Umetrics AB, Umeå, Sweden).

Solvent accessible surface areas (SASA) were computed with an in-house program using Parse radii,[43] with a probe radius of 1.4 Å and a distance between sphere points of 0.2 Å. They provide an approximate measure of the steric accessibility of each reactive group.[13,19]

**TABLE 1: Relative Activation Energies for the Oxidation with a Porphyrin Model for Both the Doublet and Quartet Spin States**

| | | energy (kJ/mol) | |
|---|---|---|---|
| | substrate[a] | doublet | quartet |
| 1 | benzene | 86.7 | 88.4 |
| 2 | nitrobenzene (o) | 79.4 | 77.9 |
| 2 | nitrobenzene (m) | 83.0 | 83.4 |
| 2 | nitrobenzene (p) | 81.2 | 78.7 |
| 3 | *N*,*N*-dimethylaniline (o) | 60.3 | 66.4 |
| 3 | *N*,*N*-dimethylaniline (m) | 85.8 | 88.8 |
| 3 | *N*,*N*-dimethylaniline (p) | 60.4 | 66.6 |
| 4 | *S*-warfarin (5) | 81.9 | 81.9 |
| 4 | *S*-warfarin (6) | 79.9 | 83.3 |
| 4 | *S*-warfarin (7) | 79.0 | 80.2 |
| 4 | *S*-warfarin (8) | 76.7 | 79.5 |
| 5 | diclofenac (4′a)[c] | 73.0 | 74.8 |
| 5 | diclofenac (4′b)[c] | 69.9 | 71.0 |
| 5 | diclofenac (5) | 69.1 | 73.8 |
| 6 | flurbiprofen (4′) | 80.4 | 81.7 |
| 7 | ethene | 75.3 | 69.5 |
| 8 | 2-butene | 62.8 | [b] |

[a] Numbers or letters in brackets indicate the position at which the oxidation takes place. [b] The calculation could not be converged. For the smaller basis set, the energy was estimated to be 0.4 kJ/mol higher than for the same reaction in the doublet spin state. [c] 4′a/4′b: For the 4′ site, we tested reactions both on the same side of (4′a) and the side opposite to (4′b) the nitrogen lone pair.

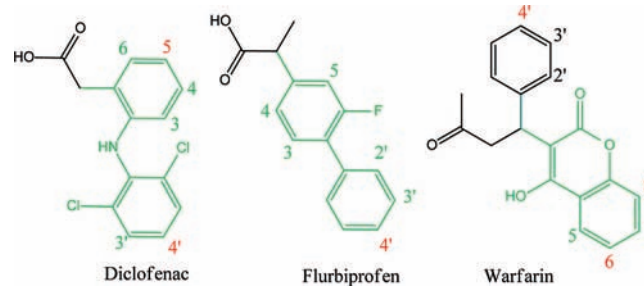


**Figure 1.** Substrates diclofenac, flurbiprofen, and warfarin. The green parts of the substrates were included in the calculations with the full compound I model. The red labels mark out the experimentally observed site of metabolisms.[44−50]

## Results

We have studied 17 different oxidation reactions (Table 1 and Figure 1). They were selected on the basis of their activation energies, the position of the substituent, and hybridization of the carbon atom involved in the oxidation reaction. For example, the $NMe_2$ and $NO_2$-substituted benzenes were selected because they gave the smallest and largest activation energies in the study

of Bathelt et al.,[24] whereas the ortho-substituted benzenes were studied because they were not included in that study. Furthermore, we wanted to include also more druglike molecules with other types of aromatic rings (e.g., the coumarin ring in warfarin) or oxidation reactions involving alkene $sp^2$-hybridized carbon atoms.

Because of the known two-state reactivity of the CYPs,[51] we studied the reactions in both the doublet and quartet spin states. The correlations presented here are to the lowest energy of the two spin states, unless otherwise stated. In Table 1, the final activation energies (relative to the isolated compound I and substrate) calculated with the BSII basis set and including zero-point vibrational energy are presented (energies with the smaller basis set and without zero-point vibrational energy are listed in Table S1 of the Supporting Information).

It can be seen that the calculated activation energies show a rather restricted variation, ranging from 60 kJ/mol for *N*,*N*-dimethylaniline to 87 kJ/mol for benzene. For aliphatic oxidations, a variation twice as large was observed (30−84 kJ/mol).[27] Moreover, the activation energies are in general higher for the aromatic oxidation than for the aliphatic oxidations (which were lower than 74 kJ/mol for all substrates except methane). This indicates that the intrinsic reactivity of aromatic group is competitive only if there are no aliphatic groups that are activated by heteroatoms (nitrogen, sulfur, or oxygen) or next to aromatic or alkene $sp^2$-hybridized carbon atoms (if one assumes that the difference between these reactions is purely enthalpic, which might not always be the case[52]).

We also see that the activation energies of the two spin states are rather similar, within 6 kJ/mol. However, the activation energy of the quartet state is somewhat higher in all except three states (nitrobenzene at the ortho and para positions, and ethene). Moreover, the activation energies of the two nonaromatic substrates are well inside the range of the range of the other substrates. Likewise, the three druglike molecules give activation energies that are within the ranges of the model compounds, showing that the latter give representative results.

As in our previous study of aliphatic hydroxylation reactions by CYPs,[28] we tried to correlate these energies to geometrical features such as the C−O and Fe−O bond lengths. However, no such correlations were found. The geometric features are more correlated to the spin states than to the energies. For example, the C−O bond lengths in the transition states are always longer in the doublet spin states than in the quartet, and they vary from 1.82 to 2.20 Å (ortho-oxidation of nitrobenzene in the quartet spin state and oxidation of 2-butene in the doublet spin state, respectively). Even within the same spin state, no correlation to the activation energies was found.

The oxidation of benzene and the meta- and para-oxidation of nitrobenzene and *N*,*N*-dimethylaniline, as well as eight other monosubstituted benzenes (chlorobenzene, anisole, cyanobenzene, fluorobenzene, toluene, thioanisole, aniline, and acetanilide), have been studied previously by Bathelt et al.[24] They used different software and basis sets, and they calculated the activation energies relative to compound I restricted to $C_s$ symmetry, resulting in 13−23 kJ/mol lower activation energies. Of these energy differences 7 kJ/mol can be attributed to the artificial $C_s$ symmetry restraint of compound I. The remaining differences are from basis sets and software difference. Both investigations use the same basis set for the nonmetal atoms in the geometry optimizations but we use an appreciably larger basis set in the energy calculations and do not use an effective core potential for the metal. Thus, our energies are not directly comparable but we get similar energy differences between the various oxidation reactions.

**TABLE 2: Correlations and Mean Absolute Deviations of DFT Calculations with the Full Compound I Model Without the Frequency or Big-Basis Calculations Compared to the Energies in Table 1**

| | doublet | quartet |
|---|---|---|
| | No frequency calculation | |
| $r^2$ | 0.98 | 0.94 |
| MAD (kJ/mol) | 0.9 | 1.4 |
| | No frequency or big-basis calculations | |
| $r^2$ | 0.95 | 0.91 |
| MAD (kJ/mol) | 1.7 | 1.9 |

**Simplified DFT Calculations.** The energies presented in Table 1 constitute state-of-the-art DFT estimates of the intrinsic activation energy for the oxidation of various substrates by compound I in the CYPs. Similar methods have been used on models of other enzymes with absolute errors of ∼20 kJ/mol and significantly smaller relative errors.[53,54] They have also been applied to CYPs,[51] giving kinetic isotope effects[55] and regioselectivities[56] in good agreement with experiment. The aim of this study is to see if we can predict these energies with faster and simpler methods.

A first step to reduce the computational time is to exclude the zero-point vibrational energies because the frequency calculations take almost as much time as the geometry optimizations. The results in Table 2 show that the frequency calculations are not really needed. The energies without zero-point energies correlate excellently with the final energies ($r^2$ is 0.94−0.98 and the MAD is 1 kJ/mol for both the doublet and quartet spin states). We can also omit the final energy calculation with the big basis set (BSII) and still get good correlations ($r^2$ of 0.91−0.95 and MADs of 2 kJ/mol). This reduces the computational time with a similar amount as omitting the frequency calculation. However, the calculations (the geometry optimizations) still take about a week.

**Smaller Models of Compound I.** It has previously been shown that the methoxy radical can be used as a model for compound I when studying the hydroxylation of aliphatic carbon atoms[28,57] as well as in semiempirical studies of hydroxylation of aromatic carbon atoms.[15,20,21,58] Therefore, we also tested how well the activation energies and the energies of the tetrahedral intermediate, calculated with the methoxy radical could reproduce the energies in Table 1. As is shown in part a of Figure 2 and Table 3, the activation energies calculated with the methoxy radical at the B3LYP/6−31G(d) level correlate well with the final DFT energies calculated with the full compound I model. Even if there is a large shift in the absolute activation energies (60 kJ/mol), $r^2$ is 0.79 and the MAD after linear regression is only 3 kJ/mol. The energies of the tetrahedral intermediate give a much worse correlation with $r^2 = 0.38$. This is partly an effect of the two nonaromatic substrates but even without them, $r^2$ is only 0.53.

We also calculated the same activation energies and energies of the tetrahedral intermediate using the semiempirical AM1 method. However, the results showed little correlation with our target DFT energies: The $r^2$ values were 0.42 and 0.35 for the activation energies and the intermediate energies, respectively (0.45 for the intermediate energies without the alkene $sp^2$ oxidations). Thus, our results show that semiempirical predictions may give unreliable results. We also calculated the energies of the transition state and the intermediate for all the substrates studied by Bathelt et al.[24] with the methoxy radical using the B3LYP and AM1 methods to ensure that our correlations are

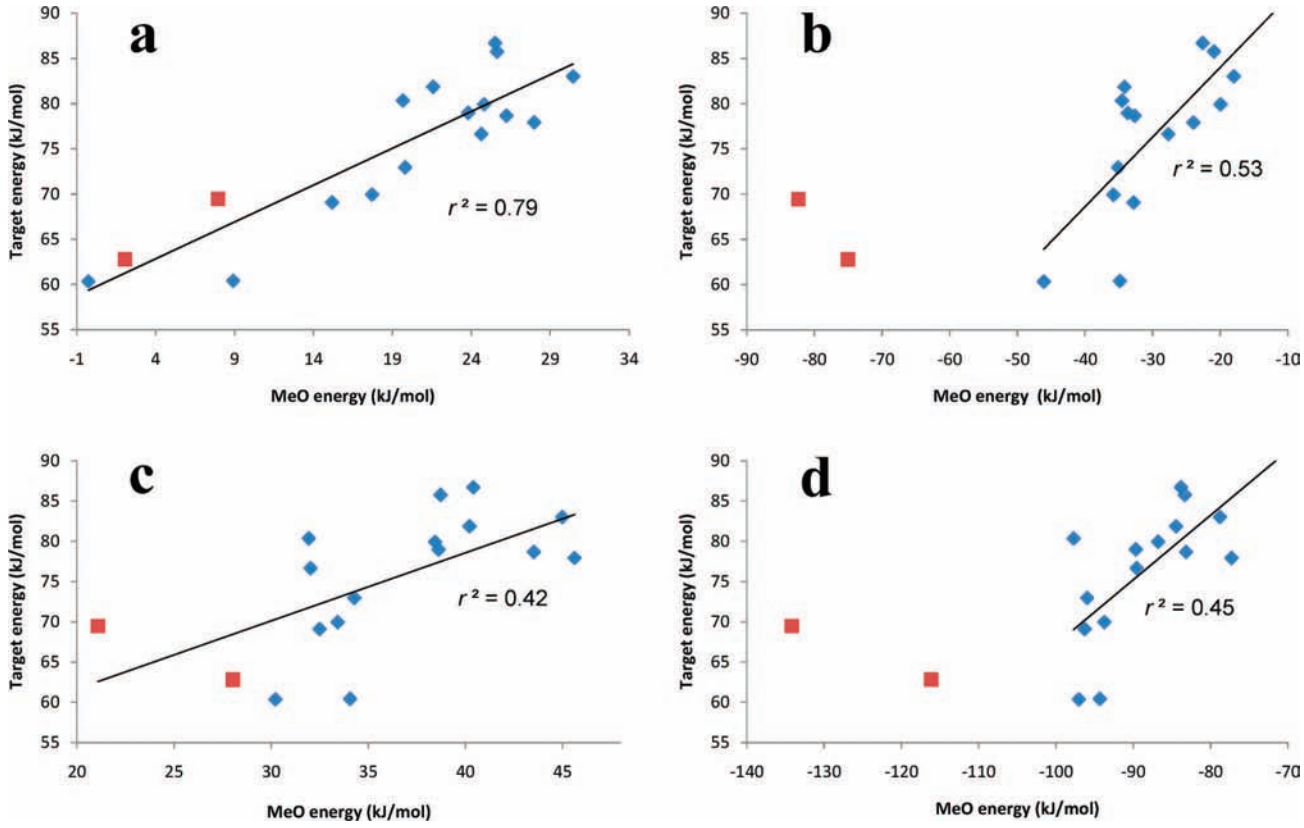


**Figure 2.** The correlation between the target DFT energies and energies calculated with a methoxy-radical model. a) Activation energy, and b) intermediate energy, both calculated at the B3LYP/6−31G(d) level. c) Activation energy, and d) intermediate energy, both calculated at the AM1 level. The energies are in kJ/mol. Data points for aromatic oxidations are shown as blue diamonds, and data points for alkene $sp^2$ oxidations are shown as red squares. The trend lines and $r^2$ values are for all data points in a) and c), whereas they exclude the nonaromatic oxidations in b) and d).

**TABLE 3: Correlations and Mean Absolute Deviations of B3LYP and AM1 Calculations with the Methoxy Radical Compared to the Lowest Activation Energies in Table 1**

| | B3LYP | | AM1 | |
|---|---|---|---|---|
| | transition state | intermediate | transition state | intermediate |
| $r^2$ | 0.79 | 0.38 | 0.42 | 0.35 |
| MAD (kJ/mol) | 3.2 | 5.0 | 5.2 | 5.3 |

**TABLE 4: Correlations ($r^2$) between the Target DFT Energies and Calculations with the Hydroxyl Model of Compound I**

| | our data set | our data set without alkene oxidations | Bathelt's data set[24] |
|---|---|---|---|
| | | B3LYP | |
| $BDE_{rad}$ | 0.43 | 0.57 | 0.64 |
| $BDE_{cat}$ | 0.34 | 0.56 | 0.55 |
| $BDE_{rad} + X \cdot BDE_{cat}$ | 0.74 | 0.69 | 0.80 |
| | | AM1 | |
| $BDE_{rad}$ | 0.36 | 0.44 | 0.40 |
| $BDE_{cat}$ | 0.39 | 0.56 | 0.55 |
| $BDE_{rad} + X \cdot BDE_{cat}$ | 0.60 | 0.52 | 0.50 |

[a] $X = 0.18$ for our data set and 0.07 for our data set without alkene oxidations and Bathelt's data set.

representative for a larger data set. Using B3LYP, the correlations (now to the DFT data of Bathelt et al.[24]) were nearly the same as for our data set (considering that this data set does not include any oxidations of alkene $sp^2$-hybridized carbon atoms), with $r^2 = 0.82$ for the transition state and $r^2 = 0.55$ for the intermediate energies. The AM1 method also gave similar correlations, with $r^2$ of 0.43 and 0.52 for the transition states and intermediates, respectively. Thus, we can quite confidently say that the AM1 method is not sufficiently accurate to study aromatic oxidation, whereas activation energies calculated for the methoxy radical with B3LYP give good predictions.

Other correlations have also been tested.[5,9,20] For example, Bathelt et al. used the bond dissociation energies (BDE) of the C−O bond in the tetrahedral intermediate using both a hydroxyl radical ($BDE_{rad}$) and a hydroxyl cation ($BDE_{cat}$) as a model of compound I. They achieved the best correlation with a combination of these two BDEs ($E^{\ddagger} \propto BDE_{rad} + 0.07*BDE_{cat}$, $r^2 = 0.82$).[24] We have tested this method using both the B3LYP (with the 6−31G(d) basis set) and the AM1 methods, and employing both our data set shown in Table 1, as well as for the data set of Bathelt et al.[24] The results are presented in Table 4, and show that both $BDE_{rad}$ and $BDE_{cat}$ alone give rather poor correlations for our test set ($r^2 = 0.34-0.43$). The result is somewhat improved if the oxidations of alkene $sp^2$-hybridized carbon atoms are excluded, as in Bathelt's data set ($r^2 = 0.40-0.64$). However, if we combine these BDEs according to the equation suggested by Bathelt and co-workers,[24] the correlation is significantly improved, at least with B3LYP ($r^2 = 0.69-0.80$). Unfortunately, the weight factor between the two terms depends quite strongly on the data set: They obtained a factor of 0.07, but for our data set, the optimum factor is 0.18, which raises $r^2$ from 0.63 to 0.74 (the correlation equation is $E^{\ddagger} = 0.311*(BDE_{rad} + 0.18*BDE_{cat}) + 159.0$). Thus, we can obtain almost as good results with the BDE results obtained by the hydroxyl model at the B3LYP level as for the activation energies obtained with the methoxy-radical model ($r^2 = 0.79$). The advantage with the former calculations is that a transition-

**TABLE 5: Prediction Accuracy of PLS Models Created from Hydroxyl Model Calculations of Our Data Set and Tested on Bathelt's Data Set with Overlapping Substrates Excluded[a]**

| | B3LYP model | AM1 model |
|---|---|---|
| model $r^2$ | 0.74 | 0.84 |
| model $Q^2$ | 0.66 | 0.69 |
| prediction $r^2$ | 0.77 | 0.81 |
| prediction MAD | 2.9 | 2.6 |

[a] MAD in kJ/mol.

state optimization is avoided. On the other hand, two calculations are required instead of one.

The results at the AM1 level are rather poor ($r^2 = 0.55$ for $BDE_{cat}$ alone, excluding nonaromatic oxidations, and $r^2 = 0.60$ for our full data set with both descriptors). However, it is significantly better and faster than energies obtained for the intermediate with the methoxy-radical model ($r^2 = 0.35-0.45$), a method that has been used in several previous studies.[15,20,21,58]

**QSAR Analysis.** To possibly improve the results obtained with the simple hydroxyl models, we investigated the O−C distances, as well as the spin and charge distributions of the radical and cation states by Mulliken population analysis (on the oxygen and carbon atoms involved in the reactions, as well as the hydrogen atom bound to the carbon atom), all calculated with both the B3LYP and AM1 methods (data listed in the Supporting Information). These data were then analyzed with multivariate analysis (with a partial least-squares model, PLS) using our data as training set (17 oxidations). For the B3LYP calculations, no PLS model gave better results than the combined hydroxyl model in Table 4. However, the AM1 correlations could be significantly improved at the cost of analyzing the spin on the carbon and oxygen atoms calculated with the hydroxyl radical and combining this with the energies, giving $r^2 = 0.84$ and a predictivity ($Q^2$) of 0.69. The final model equation is $E^{\ddagger}_{PLS} = 10.9604 - 812.886*C_{spin} + 169.276*O_{spin} - 0.160304*BDE_{rad} + 0.0651632*BDE_{cat}$.

To test these two predictions (the $BDE_{rad} + 0.18\ BDE_{cat}$ combination calculated with B3LYP and the PLS model based on AM1 data), we tested them on the substrates in Bathelt's data set that are not part of our data set (12 oxidations). Because our DFT energies are not directly comparable with those of Bathelt et al., we adjusted the energies by a constant so that the average energy was the same in the data set and in the predicted energies. As can be seen in Table 5, both models gave a similar accuracy as the B3LYP calculations of transition states with the methoxy radical. This is a valuable result because the AM1 calculations take only a minute to perform.

Results of a similar quality ($r^2 = 0.81$) could also be obtained by considering the spin density of the carbon bound to the oxygen in the hydroxyl radical complex (computed with B3LYP) but only for singly substituted benzenes (as in the data set of Bathelt et al.). We also did multivariate analysis of data from the calculations with the methoxy-radical model with both the B3LYP and AM1 methods but this did not give any improvements compared to the activation energies calculated with the same methods.

**Applications on Some Druglike Molecules.** ***Methyl-Substituted 3-Fluoro-anilines.*** Koerts et al.[12] have shown that the HOMO and HOMO-1 density distributions determined at a semiempirical level can give good correlation with experimentally observed product ratios for a series of fluorinated benzenes ($r^2 = 0.96$). However, for a series of methyl-substituted 3-fluoro-anilines (3-fluoro-aniline, 3-fluoro-2-methyl-aniline, 3-fluoro-4-methyl-aniline, and 3-fluoro-6-methyl-aniline), this correlation was weakened ($r^2 = 0.84$).[59] We used the methoxy radical on some of these substrates to see if we can predict the products with our methods. From Figure 3, it can be seen that there is a difference in the predicted product ratios for this series of compounds, depending on how the activation energies were determined. If the activation energy is calculated with the sum of the isolated reacting species as a reference ($E^{\ddagger}_{sep}$), there is no correlation with the experimental data (Figure 3). This is because the transition states for the reactions in the 2 and 6 positions are stabilized by favorable interactions between the $NH_2$ substituent of aniline and the methoxy radical. The corresponding activation energies are therefore much lower, and the metabolism is predicted to occur in the 2 or 6 positions. However, if the reactant complex is instead used as the reference ($E^{\ddagger}_{react}$), the interaction between the $NH_2$ substituent is included for both the reference and the transition state. This improves the agreement with the experimental data significantly, and $r^2 = 0.99$ is obtained, cf. Figure 3 and Table S9 in the Supporting Information. Energies obtained from the model based on the

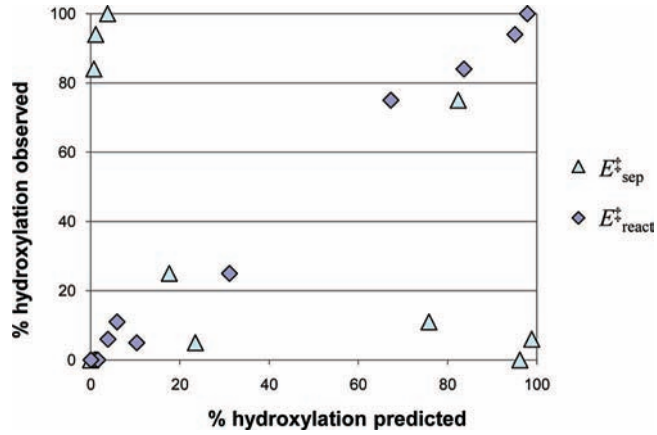


**Figure 3.** Predicted product ratios for methyl-substituted 3-fluoro-aniline compounds based on the activation energies calculated from the B3LYP methoxy-radical model. It is assumed that the product ratios are proportional to the ratios of the rate constants ($k$) and that the rate constants are related to the activation energies according to $\Delta E^{\ddagger} = -RT \ln k$ ($T = 310.15$ K).[12]

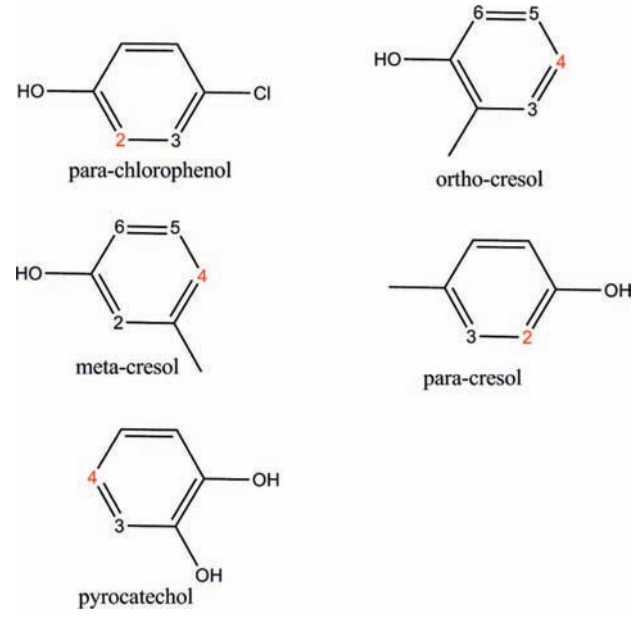


**Figure 4.** The investigated series of substituted phenols. The red labels indicate the experimentally observed sites of metabolisms.[60,61]

**TABLE 6: Solvent-Accessible Surface Area (SASA, Å²) and Calculated Activation Energies Using the Methoxy-Radical Model and the PLS Model Derived from the AM1 Descriptors for a Series of Substituted Phenols[a]**

| | | SASA (Å²) | $E^{\ddagger}_{sep}$[b] (kJ/mol) | $E^{\ddagger}_{react}$[c] (kJ/mol) | $E^{\ddagger}_{PLS}$ (kJ/mol) |
|---|---|---|---|---|---|
| *p*-Cl-phenol | **2** | 18.6 | 5.5 | 40.2 | 78.8 |
| | 3 | 16.3 | 24.1 | 35.2 | 83.4 |
| ortho-cresol | 3 | 15.5 | 24.9 | 34.2 | 83.4 |
| | **4** | 20.4 | 17.5 | 24.8 | 76.2 |
| | 5 | 20.2 | 21.9 | 29.9 | 80.6 |
| | 6 | 18.6 | 3.5 | 35.9 | 77.8 |
| meta-cresol | 2 | 13.9 | −1.1 | 31.2 | 76.4 |
| | **4** | 15.9 | 10.2 | 22.2 | 74.2 |
| | 5 | 20.0 | 28.1 | 36.8 | 85.9 |
| | 6 | 19.1 | 0.9 | 33.3 | 74.0 |
| para-cresol | **2** | 18.9 | 1.5 | 34.1 | 77.3 |
| | 3 | 15.4 | 16.2 | 27.6 | 82.4 |
| pyrocatechol | 3 | 19.2 | 3.4 | 39.4 | 82.5 |
| | **4** | 20.3 | 14.6 | 21.9 | 76.8 |

[a] Experimentally observed sites of metabolism are marked in bold face. [b] Activation energy calculated as the difference in energy between transition state and the sum of the isolated methoxy radical and substrate. [c] Activation energy calculated as the difference in energy between transition state and reactant complex.

bond dissociation energies at the B3LYP level ($BDE_{rad}$ + 0.18*$BDE_{cat}$) and the PLS model derived from the AM1 descriptors (Table S9 in the Supporting Information) also show a too large stabilization of the products that are hydroxylated in 2 or 6 positions, resulting in poor correlations ($r^2$ of 0.0 and 0.2). However, by adding a penalty of 15 kJ/mol to the positions that have favorable interactions, both these methods as well as $E^{\ddagger}_{sep}$ give good correlations (0.98, 0.98, and 0.97).

***Substituted Phenols.*** D'Yachkov et al.[21] have used the arene oxide formation estimated by semiempirical methods to predict the products for a series of benzene compounds using experimental data from many sources. We have used our methods on some of these substrates to see if we can predict the products for this set of polar substituents.

In Table 6, we see that $E^{\ddagger}_{sep}$ once again significantly underestimates the activation energy for the reactions next to hydrogen-bonding substituents (this time the OH-groups). This is not the case for $E^{\ddagger}_{react}$. However, even if $E^{\ddagger}_{react}$ gives a correct prediction of the products of three of the substrates, it still leads to wrong prediction for two of the compounds, viz. p-Cl-phenol and para-cresol. This is probably because the accessibility of the reactive carbon atom also is important, as has frequently been observed before.[17,23,28] In the two cases for which $E^{\ddagger}_{react}$ does not predict correct product, the solvent-accessible surface area (SASA) of the site with the lowest $E^{\ddagger}_{react}$ is smaller (15−16 Å²) than that of the most reactive site (19 Å²). In fact, in all cases except one (meta-cresol), the most reactive site also has the largest SASA. Thus, a combination of both $E^{\ddagger}_{react}$ and the SASA seems to be needed to obtain a correct prediction for all sites. For example, $E^{\ddagger}_{react}$ − 3*SASA provides such an estimate. The PLS model derived from the AM1 descriptors gives also relatively good results for these compounds. Even without any correction for accessibility, it gets the correct sites of metabolism for all compounds except meta-cresol, for which the observed site of metabolism is 0.2 kJ/mol too high. As above, we can add a penalty of 15 kJ/mol to the energies of the methods that do not include the reactants to improve the results. With this included, $E^{\ddagger}_{sep}$ becomes correct for all substrates except para-cresol, whereas the $E^{\ddagger}_{PLS}$ results are not improved.

***Fluoro-anilines.*** Bathelt et al.[24] have correlated activation energies determined using a porphine model with experimental rate constants ($k_{cat}$) for a set of fluorine-substituted anilines.[62] We have used the same set of compounds to validate the performance of our methods. The results in Table 7 show that both $E^{\ddagger}_{sep}$ and $E^{\ddagger}_{react}$ correlate excellently with the experimentally determined rate constants ($r^2 = 0.97-1.00$). Thus, in this case, where only para-hydroxylation is considered, it is not crucial to optimize the reactant complex to obtain agreement with the experimental data. This is important because the reactant complexes are sometimes hard to converge. Interestingly, our methoxy-radical model provides a much better correlation than the results presented by Bathelt et al.[24] ($r^2 = 0.49$), which failed to predict that 2,3,6F-aniline has the lowest rate constant and therefore the highest activation energy. Our model based on bond dissociation energies ($E^{\ddagger}_{BDE} \propto BDE_{rad} + 0.18*BDE_{cat}$) as well as the PLS model based on AM1 data also give excellent correlations with experimental data ($r^2 = 0.95-0.98$).

**TABLE 7: Correlation between Experimental $k_{cat}$ and Calculated Activation Energies (kJ/mol) Obtained with the Methoxy Radical, the Hydroxyl BDE Models, and the PLS Model Derived from the AM1 Descriptors**

| | ln $k_{cat}$ | $E^{\ddagger}_{sep}$[a] | $E^{\ddagger}_{react}$[b] | $E^{\ddagger}_{BDE}$[c] | $E^{\ddagger}_{sep}$[d] | $E^{\ddagger}_{PLS}$ |
|---|---|---|---|---|---|---|
| aniline | 5.4 | 11.4 | 18.7 | 69.7 | 48.1 | 68.3 |
| 2F-aniline | 4.5 | 12.5 | 20.0 | 70.2 | 49.0 | 71.5 |
| 2,6F-aniline | 3.3 | 14.0 | 22.2 | 71.0 | 50.2 | 75.3 |
| 2,3,6F-aniline | 1.9 | 14.8 | 24.9 | 72.5 | 49.4 | 76.9 |
| $r^2$ | | 0.97 | 1.00 | 0.98 | 0.49 | 0.95 |

[a] Activation energy calculated as the difference in energy between transition state and the sum of the isolated methoxy radical and substrate. [b] Activation energy calculated as the difference in energy between transition state and reactant complex. [c] Relative bond dissociation energies for addition of the hydroxyl radical and cation. These energies were determined as $BDE_{rad}$ and $BDE_{cat}$ and then converted to activation energies using $E^{\ddagger}_{BDE} = 0.311*(BDE_{rad} + 0.18*BDE_{cat}) + 159$. [d] Activation energy from Bathelt et al.[24] calculated with a full compound I model, converted from kcal/mol to kJ/mol.

**TABLE 8: Solvent Accessible Surface Area (SASA, Å²) and Calculated Activation Energies (kJ/mol) Using the Methoxy-Radical Model and the PLS Model Derived from the AM1 Descriptors for Diclofenac**

| site | SASA | $E^{\ddagger}_{sep}$[a] | $E^{\ddagger}_{react}$[b] | $E^{\ddagger}_{PLS}$ |
|---|---|---|---|---|
| 3′ | 15.7 | 24.3 | 34.6 | 80.2 |
| 4′ | 20.0 | 17.6 | 27.2 | 72.2 |
| 3 | 7.6 | 15.8 | 23.8 | 69.8 |
| 4 | 18.1 | 26.4 | 33.8 | 81.7 |
| 5 | 20.6 | 14.8 | 22.3 | 69.2 |
| 6 | 14.3 | 17.4 | 33.1 | 82.7 |

[a] Reaction barrier calculated as the difference in energy between transition state and the sum of the isolated methoxy radical and substrate. [b] Reaction barrier calculated as the difference in energy between transition state and reactant complex.

***Diclofenac, Flurbiprofen, and Warfarin.*** Finally we have tested our models also to three well-known substrates (Figure 1, note that the full substrates were included in these calculations). These substrates are significantly larger than the substituted benzenes and provide a test for a set of drug-like molecules.

Diclofenac is metabolized by both CYP 2C9 and 3A4, but the two enzymes give different products: 4′-hydroxy diclofenac for CYP 2C9 and 5-hydroxy diclofenac for CYP 3A4.[44] In Table 8, the SASA and the activation energies calculated with our methods are listed. It can be seen that the 4′ and 5 positions have the highest solvent accessibility and that metabolism in the 5 position has the lowest activation barrier. This agrees well

**TABLE 9: Solvent Accessible Surface Area (SASA, Å²) and Calculated Activation Energies (kJ/mol) Using the Methoxy-radical Model and the PLS Model Derived from the AM1 Descriptors for Flurbiprofen**

| site | SASA | $E^{\ddagger}_{sep}$ [a] | $E^{\ddagger}_{react}$ [b] | $E^{\ddagger}_{PLS}$ |
|---|---|---|---|---|
| 2′ | 14.1 | 11.5 | 24.2 | 82.7 |
| 3′ | 19.9 | 25.8 | 32.6 | 86.3 |
| 4′ | 20.1 | 20.3 | 27.2 | 74.8 |
| 3 | 14.3 | 25.2 | 38.5 | 84.0 |
| 4 | 14.4 | 19.4 | 30.8 | 80.7 |
| 6 | 8.8 | 23.2 | 42.2 | 82.8 |

[a] Activation energy calculated as the difference in energy between transition state and the sum of the isolated methoxy radical and substrate. [b] Activation energy calculated as the difference in energy between transition state and reactant complex.

**TABLE 10: Solvent Acessible Surface Area (SASA, Å²) and Calculated Activation Energies (kJ/mol) Using the Methoxy-Radical Model and the PLS Model Derived from the AM1 Descriptors for Warfarin**

| site | SASA | $E^{\ddagger}_{sep}$ [a] | $E^{\ddagger}_{react}$ [b] | $E^{\ddagger}_{PLS}$ |
|---|---|---|---|---|
| 2′ | 13.7 | 17.3 | 19.9 | 80.8 |
| 3′ | 20.1 | 24.3 | 31.3 | 81.8 |
| 4′ | 19.9 | 22.5 | 29.5 | 78.1 |
| 5 | 16.7 | −16.0 | 31.9 | 79.9 |
| 6 | 19.9 | 23.3 | 33.9 | 80.2 |
| 7 | 19.5 | 22.7 | 33.3 | 76.8 |
| 8 | 19.0 | 24.6 | 35.6 | 75.0 |

[a] Activation energy calculated as the difference in energy between transition state and the sum of the isolated methoxy radical and substrate. [b] Activation energy calculated as the difference in energy between transition state and reactant complex.

with the fact that CYP 3A4 has a larger active-site cavity than the other CYP enzymes[63] and therefore may be capable of orienting the substrate so that the easiest reaction occurs. It also agrees with the fact that, if the carboxylic acid group is removed from diclofenac, also the CYP 2C enzymes give almost exclusively 5-hydroxylation, indicating that this is actually the intrinsically most reactive site.[44]

For flurbiprofen, Table 9 shows that the most accessible sites are 3′ and 4′. The methoxy-radical and PLS models both predict that the 4′ position has a lower activation energy than the 3′ position, in agreement with experimental data.[45,46]

Warfarin (both the *S* and *R* enantiomers) is metabolized by aromatic hydroxylation in the 4′ position of the phenyl ring and the 6, 7, and 8 positions in the coumarin ring.[47−50] Table 10 shows that 3′ and 4′ are the most exposed positions in the phenyl ring, and both the methoxy-radical and PLS models predict that the activation energy is lower for the 4′ position than for the 3′ position, in agreement with the experimental data. In the coumarin ring, positions 6, 7, and 8 are more accessible than the 5 position, and both $E^{\ddagger}_{react}$ and $E^{\ddagger}_{PLS}$ are similar (within 5 kJ/mol) for the four sites. Therefore, metabolism is only observed in the 6, 7, and 8 positions. Once again, $E^{\ddagger}_{react}$ − 3*SASA and $E^{\ddagger}_{PLS}$ − 3*SASA give correct predictions of the sites of metabolism.

## Conclusions

We have determined the transition state for the aromatic oxidation of sixteen sites on eight substrates by a realistic model of compound I in the CYPs using state-of-the-art DFT calculations. This set of substrates includes benzene, monosubstituted benzenes, aromatic ring systems with more than one substituent, including three druglike molecules, and alkenes. We have then in a systematic manner tested if these results can be reproduced by other, computationally less demanding methods. The methods were also tested on the data set of monosubstituted benzenes studied by Bathelt and co-workers.[24]

First, we showed that both the frequency calculations and the energy calculations with a large basis set can be omitted. This reduces the computational time by ∼70% without significantly deteriorating the results ($r^2 = 0.91-0.95$ and the MADs are 2 kJ/mol).

Second, we tested if we could reproduce the full DFT results using a much smaller methoxy-radical model, studying either the transition state or the tetrahedral intermediate with both DFT and the semiempirical AM1 method. Of these four combinations, only the activation energy computed at DFT level gave a significant correlation ($r^2 = 0.79$, MAD = 3.2 kJ/mol). Thus, our results show that semiempirical predictions, which have been used in previous studies,[15,20,21] may give unreliable results.

Third, we tried to use hydroxyl-radical and the hydroxyl-cation models of compound I instead. The C−O bond dissociation energy in the tetrahedral intermediate, calculated by either model, did not give any good correlations ($r^2 = 0.56-0.64$). However, if the two energies are combined, we got a significant improvement at the DFT level ($r^2 = 0.74$ and MAD = 3.4 kJ/mol). Although such a combination requires two calculations, this still leads to a significant reduction in computational time compared to the full compound I model, reducing the time from about a week to 1−9 h.

Fourth, we use multivariate analysis on energies and properties of the tetrahedral intermediate with the methoxy-radical and hydroxyl models. This showed that, using the hydroxyl model, the AM1 results can be significantly improved using a PLS model, resulting in $r^2$ of 0.84 and a predictivity of 0.69.

Finally, we applied the B3LYP methoxy-radical and AM1 PLS models on several systems for which experimental data are available.[12,44−50,62] Our results show the site of oxidation is in general determined by two factors: the solvent-accessibility and the intrinsic reactivity (the activation energy) of the site. For the methyl-substituted F-anilines, substituted phenols, and the three druglike molecules, all but one of the reactions occur for carbon atoms with SASA > 18 Å², and among these the reactions with the lowest activation energies are also observed experimentally. In fact, the combination $E^{\ddagger}_{react}$ − 3* SASA correctly predicts the site of metabolism in all tested systems. Thus the methoxy-radical model can be used to predict the intrinsic activation energy in the reaction of aromatic and alkene $sp^2$-hybridized carbon atoms with compound I in CYPs.

**Acknowledgment.** This work was supported by grants from the Carlsberg Foundation, the Benzon Foundation, and the Swedish Research Council. It has also been supported by computer resources from Lunarc at Lund University.

**Supporting Information Available:** Energies calculated with Fe(porphine)($SCH_3$)O, methoxy-radical, hydroxyl-radical, and hydroxyl-cation models with B3LYP and AM1. Data used in QSAR analysis and predictions. This material is available free of charge via the Internet at http://pubs.acs.org.

## References and Notes

(1) Guengerich, F. P. *Chem. Res. Toxicol.* **2001**, *14*, 611–650.
(2) Korzekwa, K. R.; Swinney, D. C.; Trager, W. F. *Biochemistry* **1989**, *28*, 9019–9027.
(3) Rietjens, I. M. C. M.; Soffers, A. E. M. F.; Veeger, C.; Vervoort, J. *Biochemistry* **1993**, *32*, 4801–4812.
(4) Burka, L. T.; Plucinski, T. M.; Macdonald, T. L. *Proc. Nat. Acad. Sci. U.S.A.* **1983**, *80*, 6680–6684.

(5) Korzekwa, K.; Trager, W.; Gouterman, M.; Spangler, D.; Loew, G. H. *J. Am. Chem. Soc.* **1985**, *107*, 4273–4279.
(6) de Visser, S. P.; Ogliaro, F.; Harris, N.; Shaik, S. *J. Am. Chem. Soc.* **2001**, *123*, 3037–3047.
(7) de Visser, S. P.; Shaik, S. *J. Am. Chem. Soc.* **2003**, *125*, 7413–7424.
(8) Kumar, D.; de Visser, S. P.; Shaik, S. *Chem.—Eur. J.* **2005**, *11*, 2825–2835.
(9) Pudzianowski, A. T.; Loew, G. H. *Int. J. Quantum Chem.* **1983**, *23*, 1257–1268.
(10) Bathelt, C. M.; Ridder, L.; Mulholland, A. J.; Harvey, J. N. *J. Am. Chem. Soc.* **2003**, *125*, 15004–15005.
(11) Guroff, G.; Daly, J. W.; Jerina, D. M.; Renson, J.; Witkop, B.; Udenfrie, S. *Science* **1967**, *157*, 1524–1530.
(12) Koerts, J.; Soffers, A. E. M. F.; Vervoort, J.; De Jager, A.; Rietjens, I. M. C. M. *Chem. Res. Toxicol.* **1998**, *11*, 503–512.
(13) de Graaf, C.; Vermeulen, N. P. E.; Feenstra, K. A. *J. Med. Chem.* **2005**, *48*, 2725–2755.
(14) Cruciani, G.; Carosati, E.; De Boeck, B.; Ethirajulu, K.; Mackie, C.; Howe, T.; Vianello, R. *J. Med. Chem.* **2005**, *48*, 6970–6979.
(15) Jones, J. P.; Mysinger, M.; Korzekwa, K. R. *Drug Metab. Dispos.* **2002**, *30*, 7–12.
(16) Vermeulen, N. P. E. *Curr. Top. Med. Chem.* **2003**, *3*, 1227–1239.
(17) Afzelius, L.; Arnby, C. H.; Broo, A.; Carlsson, L.; Isaksson, C.; Jurva, U.; Kjellander, B.; Kolmodin, K.; Nilsson, K.; Raubacher, F.; Weidolf, L. *Drug Metab. Rev.* **2007**, *39*, 61–86.
(18) Oh, W. S.; Kim, D. N.; Jung, J.; Cho, K. H.; No, K. T. *J. Chem. Inf. Model.* **2008**, *48*, 591–601.
(19) Feenstra, K. A.; Starikov, E. B.; Urlacher, V. B.; Commandeur, J. N. M.; Vermeulen, N. P. E. *Protein Sci.* **2007**, *16*, 420–431.
(20) Borodina, Y.; Rudik, A.; Filimonov, D.; Kharchevnikova, N.; Dmitriev, A.; Blinova, V.; Poroikov, V. *J. Chem. Inf. Comput. Sci.* **2004**, *44*, 1998–2009.
(21) D'Yachkov, P. N.; Kharchevnikova, N. V.; Dmitriev, A. V.; Kuznetsov, A. V.; Poroikov, V. V. *Int. J. Quantum Chem.* **2007**, *107*, 2454–2478.
(22) Korzekwa, K. R.; Jones, J. P.; Gillette, J. R. *J. Am. Chem. Soc.* **1990**, *112*, 7042–7046.
(23) Singh, S. B.; Shen, L. Q.; Walker, M. J.; Sheridan, R. P. *J. Med. Chem.* **2003**, *46*, 1330–1336.
(24) Bathelt, C. M.; Ridder, L.; Mulholland, A. J.; Harvey, J. N. *Org. Biomol. Chem.* **2004**, *2*, 2998–3005.
(25) de Visser, S. P.; Ogliaro, F.; Shaik, S. *Angew. Chem., Int. Ed.* **2001**, *40*, 2871–2874.
(26) Shaik, S.; de Visser, S. P.; Ogliaro, F.; Schwarz, H.; Schroder, D. *Curr. Opin. Chem. Biol.* **2002**, *6*, 556–567.
(27) de Visser, S. P.; Kumar, D.; Shaik, S. *J. Inorg. Biochem.* **2004**, *98*, 1183–1193.
(28) Olsen, L.; Rydberg, P.; Rod, T. H.; Ryde, U. *J. Med. Chem.* **2006**, *49*, 6489–6499.
(29) Ogliaro, F.; Filatov, M.; Shaik, S. *Eur. J. Inorg. Chem.* **2000**, 2455–2458.
(30) Becke, A. D. *Phys. Rev. A* **1988**, *38*, 3098–3100.
(31) Lee, C. T.; Yang, W. T.; Parr, R. G. *Phys. Rev. B* **1988**, *37*, 785–789.
(32) Becke, A. D. *J. Chem. Phys.* **1993**, *98*, 5648–5652.
(33) Dewar, M. J. S.; Zoebisch, E. G.; Healy, E. F.; Stewart, J. J. P. *J. Am. Chem. Soc.* **1985**, *107*, 3902–3909.
(34) Schafer, A.; Horn, H.; Ahlrichs, R. *J. Chem. Phys.* **1992**, *97*, 2571–2577.
(35) Hehre, W. J.; Ditchfield, R.; Pople, J. A. *J. Chem. Phys.* **1972**, *56*, 2257–2261.
(36) Hariharan, P. C.; Pople, J. A. *Theor. Chim. Acta* **1973**, *28*, 213–222.
(37) Francl, M. M.; Pietro, W. J.; Hehre, W. J.; Binkley, J. S.; Gordon, M. S.; Defrees, D. J.; Pople, J. A. *J. Chem. Phys.* **1982**, *77*, 3654–3665.
(38) Frisch, M. J.; Pople, J. A.; Binkley, J. S. *J. Chem. Phys.* **1984**, *80*, 3265–3269.
(39) Rulisek, L.; Jensen, K. P.; Lundgren, K.; Ryde, U. *J. Comput. Chem.* **2006**, *27*, 1398–1414.
(40) Ahlrichs, R.; Bar, M.; Haser, M.; Horn, H.; Kolmel, C. *Chem. Phys. Lett.* **1989**, *162*, 165–169.
(41) Treutler, O.; Ahlrichs, R. *J. Chem. Phys.* **1995**, *102*, 346–354.
(42) *Gaussian 03*, Revision C.02; Gaussian, Inc.: Wallingford CT, 2004.
(43) Sitkoff, D.; Sharp, K. A.; Honig, B. *J. Phys. Chem.* **1994**, *98*, 1978–1988.
(44) Mancy, A.; Antignac, M.; Minoletti, C.; Dijols, S.; Mouries, V.; Duong, N. T. H.; Battioni, P.; Dansette, P. M.; Mansuy, D. *Biochemistry* **1999**, *38*, 14264–14270.
(45) Tracy, T. S.; Rosenbluth, B. W.; Wrighton, S. A.; Gonzalez, F. J.; Korzekwa, K. R. *Biochem. Pharmacol.* **1995**, *49*, 1269–1275.
(46) Tracy, T. S.; Marra, C.; Wrighton, S. A.; Gonzalez, F. J.; Korzekwa, K. R. *Biochem. Pharmacol.* **1996**, *52*, 1305–1309.
(47) Kaminsky, L. S.; Demorais, S. M. F.; Faletto, M. B.; Dunbar, D. A.; Goldstein, J. A. *Mol. Pharmacol.* **1993**, *43*, 234–239.
(48) Rettie, A. E.; Korzekwa, K. R.; Kunze, K. L.; Lawrence, R. F.; Eddy, A. C.; Aoyama, T.; Gelboin, H. V.; Gonzalez, F. J.; Trager, W. F. *Chem. Res. Toxicol.* **1992**, *5*, 54–59.
(49) Yamazaki, H.; Shimada, T. *Biochem. Pharmacol.* **1997**, *54*, 1195–1203.
(50) Zhang, Z.; Fasco, M. J.; Huang, Z.; Guengerich, F. P.; Kaminsky, L. S. *Drug Metab. Dispos.* **1995**, *23*, 1339–1345.
(51) Shaik, S.; Kumar, D.; de Visser, S. P.; Altun, A.; Thiel, W. *Chem. Rev.* **2005**, *105*, 2279–2328.
(52) Takahashi, A.; Kurahashi, T.; Fujii, H. *Inorg. Chem.* **2007**, *46*, 6227–6229.
(53) Himo, F.; Siegbahn, P. E. M. *Chem. Rev.* **2003**, *103*, 2421–2456.
(54) Siegbahn, P. E. M.; Blomberg, M. R. A. *Chem. Rev.* **2000**, *100*, 421–437.
(55) Li, C. S.; Wu, W.; Kumar, D.; Shaik, S. *J. Am. Chem. Soc.* **2006**, *128*, 394–395.
(56) Park, J. Y.; Harris, D. *J. Med. Chem.* **2003**, *46*, 1645–1660.
(57) Higgins, L.; Korzekwa, K. R.; Rao, S.; Shou, M. G.; Jones, J. P. *Arch. Biochem. Biophys.* **2001**, *385*, 220–230.
(58) Dowers, T. S.; Rock, D. A.; Rock, D. A.; Perkins, B. N. S.; Jones, J. P. *Drug Metab. Dispos.* **2004**, *32*, 328–332.
(59) Koerts, J.; Boeren, S.; Vervoort, J.; Weiss, R.; Veeger, C.; Rietjens, I. M. C. M. *Chemico-Biological Interactions* **1996**, *99*, 129–146.
(60) Parke, D. V. *The Biochemistry of Foreign Compounds*; Pergamon Press: Oxford, 1968.
(61) Williams, R. T. *Detoxication Mechanisms. The Metabolism and Detoxication of Drugs, Toxic Substances and Other Organic Compounds*; Chapman & Hall: London, 1959.
(62) Cnubben, N. H. P.; Peelen, S.; Borst, J. W.; Vervoort, J.; Veeger, C.; Rietjens, I. M. C. M. *Chem. Res. Toxicol.* **1994**, *7*, 590–598.
(63) Ekroos, M.; Sjögren, T. *Proc. Nat. Acad. Sci. U.S.A.* **2006**, *103*, 13682–13687.

JP803854V